Materials Transactions, Vol. 45, No. 7 (2004) pp. 2012 to 2017
Special Issue on Grain Boundaries, Interfaces, Defects and Localized Quantum Structures in Ceramics

HRTEM and EELS Studies of $L1_0$-Ordered FePt nano-Clusters on MgO Films Prepared Below 673 K

Shunsuke Fukami[1,*1], Akichika Ohno[1,*1] and Nobuo Tanaka[1,2,*2]

[1]*Department of Crystalline Materials Science, Nagoya University, Nagoya 464-8603, Japan*
[2]*EcoTopia Science Institute, Nagoya University, Nagoya 464-8603, Japan*

Three kinds of FePt-MgO granular films were prepared by a vacuum successive deposition of MgO, Pt, Fe and MgO on a cleaved surface of sodium chloride below 673 K. Their microstructures, electronic structures and magnetic properties were studied by high-resolution transmission electron microscopy (HRTEM), electron energy-loss spectroscopy (EELS) and measurement with a superconducting quantum interference device (SQUID) magnetometer. The TEM observations and selected area electron diffraction patterns revealed that the samples mainly consist of few nm-sized FePt clusters embedded in MgO films with $L1_0$-ordered structure and *c*-axis perpendicular to the film surface. Size effect on the stability of $L1_0$ phase in the FePt nano-clusters was directly observed in [MgO/Fe(0.38 nm)/Pt(0.30 nm)/MgO] and the critical size of the transition from $L1_0$ to A1 phase was estimated as around 2 nm, that can be considered as smaller than effective size for the transition from ferromagnetism to superparamagnetism. Coercivity of [MgO/Fe(1.0 nm)/Pt(0.8 nm)/MgO] was 1.2×10^5 A/m. The Fe-$L_{2,3}$ white-line ratios of the present samples measured by EELS were about 4.0, independently on the incident direction of electron beam. The higher white-line ratio may be attributed to their high-spin state by a change of 3d-band structure owing to the hybridization of d-bands between Fe and Pt atoms.

(Received January 19, 2004; Accepted March 10, 2004)

Keywords: *perpendicular magnetic recording media, $L1_0$-iron platinum, nano-cluster, high-resolution transmission electron microscopy, electron energy-loss spectroscopy, size-effect, low temperature preparation, magnesium oxide, white-line ratio*

1. Introduction

Area-density of magnetic recording has been increasing year by year and in the near future, superparamagnetism of the recording units will become a serious problem because each bit must scale down into nano-meter range. $L1_0$-FePt is one of the strong candidates for future high-density magnetic recording media due to its very high magnetocrystalline anisotropy along the *c*-axis ($K_u = 6.6$–10×10^6 J/m^3)[1)] which can overcome the thermal agitation and the realization of perpendicular magnetic recording[2)] by controlling the crystal axis properly. This fact gives us a great advantage for high-density magnetic recording. Isolation of each of the magnetic grains for keeping the suitable signal to noise ratio is also crucial for high-density recording. From these viewpoints, many studies on the preparation of granular films, in which FePt nano-clusters are dispersed in non-magnetic matrix, have been carried out in recent years.[3–6)] Bian *et al.* successfully prepared FePt nanoparticles around 10 nm diameter by vacuum successive deposition technique of Pt, Fe and Al_2O_3 on a (001) surface of sodium chloride, however $L1_0$-FePt was formed with three kinds of variant, one of which has *c*-axis perpendicular to film surface after annealing at 873 K.[3)] Other studies also needed high temperature for forming $L1_0$ phase. For the practical application, process temperature should be suppressed lower and a few researches have been reported from this viewpoint.[7,8)]

In the present paper, we prepared FePt-MgO granular films below 673 K, in which nano-meter sized $L1_0$-FePt clusters are dispersed inside MgO films and *c*-axis of each clusters are aligned perpendicular to the film plane. Then microstructure and electronic structure are investigated by high-resolution transmission electron microscopy (HRTEM) and electron energy-loss spectroscopy (EELS), respectively. EELS can be generally used for characterizing compositions and electronic structures of solid matters[9)] and gives similar result by X-ray absorption spectroscopy (XAS). L_2 and L_3 edges seen in the spectrum of transition metal, which are originated from the transition of $2p_{1/2}$ and $2p_{3/2}$ to unoccupied 3d-band, respectively, have information about 3d-band structure.[10,11)] Intensity ratio of L_3 to L_2, L_3/L_2, is called as a white-line ratio, which is changed by core-hole interaction and gives much information about oxidation state, valency or spin state of the transition metals.[12,13)] Magnetic properties were measured, and size effect on the stability of $L1_0$ phase, which was recently studied,[14–16)] is also discussed for the interpretation of the experimental results.

2. Experimental Procedures

FePt-MgO granular films were prepared by ultra high vacuum deposition technique. First, under a base pressure of 6.7×10^{-6} Pa, MgO was deposited 15 nm thickness using an electron beam heating on a cleaved NaCl (001) surface kept at 573 K. Then Pt, Fe and MgO (8 nm) were deposited successively on the MgO film at 673 K. Pt and Fe were evaporated from another electron beam heating source and a resistance heating one, respectively. The average thickness was estimated with a quartz thickness monitor attached near the substrate and the thicknesses of Pt and Fe were controlled to equiatomic ratio. Deposition rates were about 10, 0.1 and 1 nm/min. for MgO, Pt and Fe, respectively. After the deposition, sample was kept at 673 K for about 10 minutes, and then cooled gradually at a rate of 10-20 K/min.

For TEM observations and EELS measurements, NaCl substrates were removed in distilled water and MgO/Fe/Pt/MgO films of around 25 nm total thickness were mounted on

*1Graduate Student, Nagoya University
*2Corresponding author, E-mail: a41263a@nucc.cc.nagoya-u.ac.jp

carbon grids supported by copper meshes. TEM observations and EELS measurements were performed with 200 kV TEM (JEM-2010) and 300 kV TEM (TECNAI F30) with a post column energy filter (Gatan Imaging Filter), respectively. Energy drifts of EELS were corrected by a dedicated software.[17] Magnetic properties were measured with a superconducting quantum interference device (SQUID) magnetometer.

3. Results and Discussions

In the present study, we have prepared three kinds of samples, which are different each in the thickness of Pt and Fe. Figure 1 shows TEM images and selected area electron diffraction (SAED) patterns of them. Figures 1(a) and (b) of [MgO/Fe(1.0 nm)/Pt(0.8 nm)/MgO], (c) and (d), [MgO/Fe-(0.77 nm)/Pt(0.60 nm)/MgO], and (e) and (f), [MgO/Fe-(0.38 nm)/Pt(0.30 nm)/MgO].

In the SAED patterns, we can clearly see 110 spots of FePt as well as the strong fundamental reflections. These are superlattice reflections meaning the existence of $L1_0$-ordered phase. It is found that FePt and MgO have a certain epitaxial orientation, *i.e.* $[100](001)_{FePt} \parallel [100](001)_{MgO}$ with the *c*-axis normal to the film surface, which is ideal for the perpendicular magnetic recording.

In the TEM images, it is found that few nano-meter size clusters are dispersed two-dimensionally. From the statistics of more than 100 clusters, the average diameter of clusters are obtained as 7.1 nm, 4.5 nm and 2.9 nm for [MgO/Fe(1.0 nm)/Pt(0.8 nm)/MgO], [MgO/Fe(0.77 nm)/Pt(0.60 nm)/MgO] and [MgO/Fe(0.38 nm)/Pt(0.30 nm)/MgO], respectively. We can see Moiré fringes in the clusters, whose spacings are consistent with the interference between the lattice spacing of $L1_0$-FePt and MgO. Also, comparing the 110 dark field TEM image with the bright field TEM image, we concluded that large part of the FePt clusters are in the ordered phase and in the above epitaxial orientations. Moreover, a previous report using nano-beam EDS showed that the composition of Fe and Pt in a sample fabricated in a similar way to the present experiment is almost as same as the deposited composition and its difference from particle to particle is within a standard deviation of 3 at%Pt,[18] which expect us that the composition of each of the present particles is 50 ± 5 at%Pt, in the range of $L1_0$ ordered phase.

Figure 2 shows HRTEM images of typical clusters in each sample as shown in Fig. 1. Because {110} lattice fringes are clearly seen in all over the clusters, they are considered to consist of a single valiant with the $L1_0$-ordered phase and the above epitaxial relation. This fact is different from the previous FePt samples reported by Bian *et al.*[3] This difference may come from an MgO underlayer. We used the MgO underlayer for growth of FePt, which consists of face centered cubic structure and whose lattice constant is 0.421 nm. This underlayer can be considered to effectively align the *c*-axis of FePt clusters normal to the film surface by the small lattice misfit. ($\eta = (d_{FePt(100)} - d_{MgO(100)})/d_{MgO(100)} = -8.5\%$.)

Figure 3 shows the HRTEM image of another area in [MgO/Fe(0.38 nm)/Pt(0.30 nm)/MgO]. In this micrograph, there are two clusters, one is about 2.7 nm in diameter (the upper side) and another is about 1.5 nm in diameter (the lower side). While {110} lattice fringes of $L1_0$-FePt are

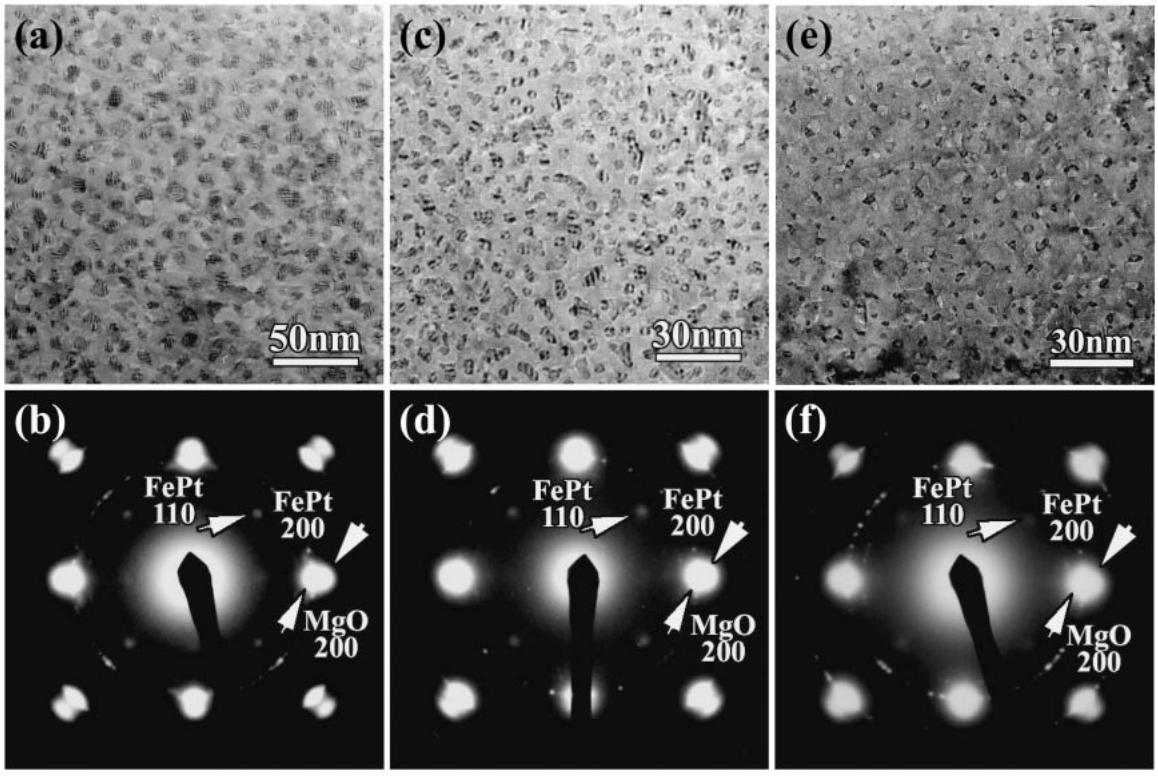

Fig. 1 TEM images and SAED patterns of (a), (b) [MgO/Fe(1.0 nm)/Pt(0.8 nm)/MgO], (c), (d) [MgO/Fe(0.77 nm)/Pt(0.60 nm)/MgO], (e), (f) [MgO/Fe(0.38 nm)/Pt(0.30 nm)/MgO].

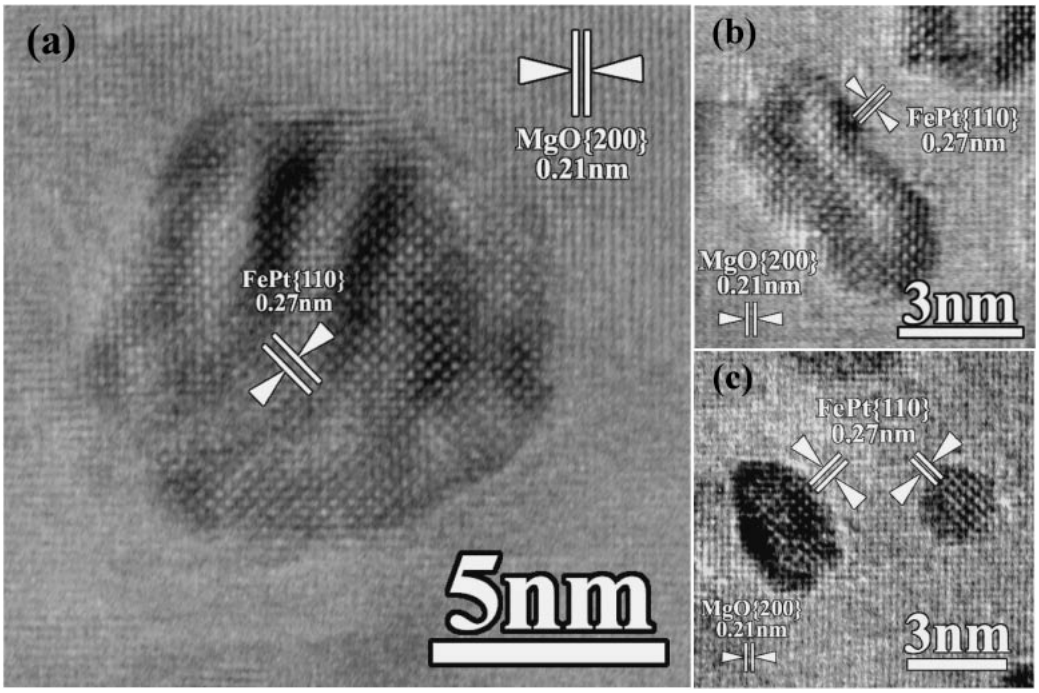

Fig. 2 HRTEM images of (a) [MgO/Fe(1.0 nm)/Pt(0.8 nm)/MgO], (b) [MgO/Fe(0.77 nm)/Pt(0.60 nm)/MgO] and (c) [MgO/Fe(0.38 nm)/Pt(0.30 nm)/MgO].

clearly seen in the upper cluster, only {200} lattice fringes of disorder-FePt are seen in the lower one. Even by defocusing, no lattice fringe related with the ordered structures appeared in the lower cluster. This means that the lower cluster is in a disordered-A1 phase, while the upper one is sufficiently ordered. From the intensive observations of other many clusters, we could conclude that clusters less than around 2 nm diameters are reluctant to order. This result shows the direct evidence of the size effect on the stability of $L1_0$-ordered phase, that is to say, FePt ultra-fine particles smaller than a certain size adopt A1-disorder phase rather than $L1_0$-ordered phase even at low temperature.[14–16] Then, our interest focuses on which is critical for ferromagnetism in FePt clusters, structural transition of hard magnetic $L1_0$ phase to soft magnetic A1 phase or magnetic phase transition of ferromagnetism to superparamagnetism. Kitakami and Shimada estimated the threshold diameter of ferromagnetism-superparamagnetism transition as around 2.8 nm.[19,20] Takahashi *et al.* suggested that FePt particles smaller than ~4 nm are not ordered to the $L1_0$ structure.[14] In the present study, however, we prepared FePt clusters smaller than 2.8 nm diameter with $L1_0$-ordering as shown in Fig. 2(c) and Fig. 3. Therefore we can conclude that the present preparation method enables us to exceed the size limit of magnetic phase transition, and as the result, superparamagnetism is a more critical factor for establishing FePt nano-magnets.

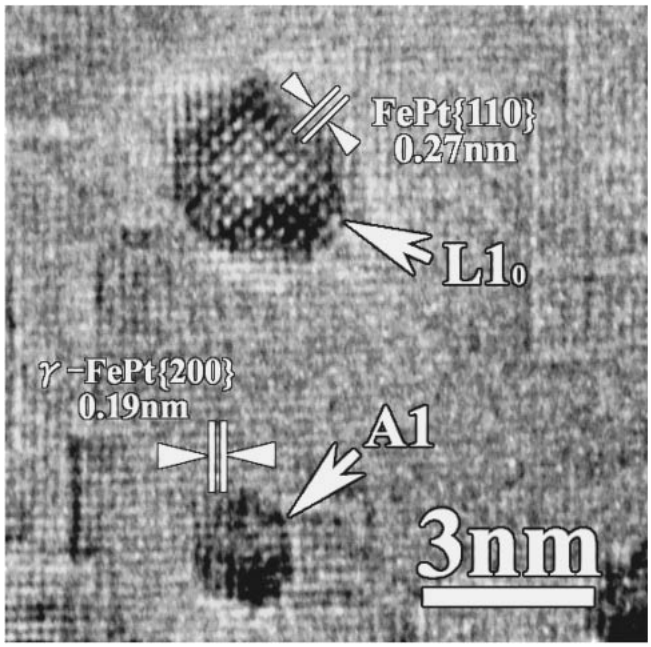

Fig. 3 HRTEM image of [MgO/Fe(0.38 nm)/Pt(0.30 nm)/MgO]. The upper cluster is in $L1_0$-order phase whereas the under one is in A1-disorder phase. This indicates the size effect on the stability of $L1_0$ phase.

Figure 4 shows the magnetization curve of [MgO/Fe(1.0 nm)/Pt(0.8 nm)/MgO] measured at 5 K where an external field was applied normal to the film. Coercivity of the present sample is 1.2×10^5 A/m, but its hysterisis shape is somewhat different from the normal one. As a simple model, we could guess that two phases, one is magnetically hard phase, that is $L1_0$-FePt in this case, and another is soft phase such as disorder FePt or pure Fe, coexist in the present samples. Although the coercivity is not so large, we may be able to gain larger coercivity if we can prepare the films predominantly consist of hard phase, as is one of our future objects.

In the next, we studied electronic structures relating to magnetism of clusters using EELS in TEM. The EELS data show occupancy of 3d-band of iron atoms in FePt clusters. Figure 5 shows the Fe-$L_{2,3}$ edges in the EELS measured from

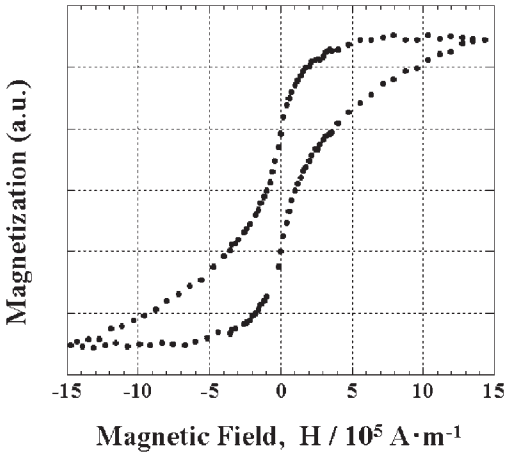

Fig. 4 Magnetization curve of [MgO/Fe(1.0 nm)/Pt(0.8 nm)/MgO] measured at 5 K where external field was applied normal to the film. Coercivity is 1.2×10^5 A/m.

the present three samples, where backgrounds of the spectra were subtracted by following way.

(1) Subtract using an AE^{-r} fit over an energy interval extending around 50 eV before the Fe-$L_{2,3}$ edge, where A and r are arbitrary constant and E means loss-energy.
(2) For the continuous ionization background after L_3 edge, subtract a curve which is zero at the peak of L_3 edge and connects smoothly with post edge.

It might be true that we should subtract the background using the hydrogenic model[9] for the process of (2) in the case that the energy resolution was enough, but the present way seems to be a good approximation because the white-line ratios obtained from the present method are, within order of 0.01, different from those from using the hydrogenic model. The white-line ratios thus determined are 4.0, 4.0 and 3.9 for [MgO/Fe(1.0 nm)/Pt(0.8 nm)/MgO], [MgO/Fe(0.77 nm)/Pt(0.60 nm)/MgO] and [MgO/Fe(0.38 nm)/Pt(0.30 nm)/MgO], respectively. These values are considered to be significantly bigger than that of pure Fe, white-line ratio of which equals to 3.0.[12]

Figure 6 shows the Fe-$L_{2,3}$ edges in EELS of (a) [MgO/Fe(1.0 nm)/MgO] and (b) [MgO/Fe(2.0 nm)/MgO] prepared in perfectly the same condition with the present FePt samples, only the difference is whether there is Pt or not. The structure and texture of the Fe in these samples were confirmed to be an α-Fe and dispersed as nano-clusters like FePt samples by TEM observations and SAED patterns. The white-line ratios of these samples are obtained as 3.4 and 3.2 for [MgO/Fe(1.0 nm)/MgO] and [MgO/Fe(2.0 nm)/MgO], respectively.

Now, we discuss why the white-line ratios obtained from FePt clusters samples became bigger than those from pure Fe. First of all, various kinds of iron oxides are known to show relatively higher white-line ratio, for example it becomes 4.1 for FeO and more than 5.0 for Fe_2O_3.[12,21] If a part of Fe in [MgO/Fe/Pt/MgO] samples is oxidized and only the oxidation phase influenced to high white-line ratio, the above [MgO/Fe/MgO] samples must show higher white-line ratio than [MgO/Fe/Pt/MgO] samples because Fe atoms in [MgO/Fe/MgO] cannot alloy with Pt atoms. However, the white-line ratios of Fe-L edge in [MgO/Fe/MgO], actually, remain slightly higher value than that of pure Fe. We can consequently conclude that Fe in $L1_0$-FePt intrinsically shows the high white-line ratio. The possible factors to enhance the white-line ratio are considered as followings. Now, we refer three previous studies related to the present issue. First, Thole and Laan suggested that high-spin states have on average a larger white-line ratio than a low-spin state.[22] Next, Sakuma described that the strong K_u of $L1_0$-FePt should be partly attributed to the hybridization of d-bands between Fe and Pt atoms.[23] Finally, Morrison *et al.* studied amorphous FeGe alloy, and concluded that the smaller white-line ratio of FeGe than pure Fe originates from the lower-spin state brought about by the hybridization of d-band.[11] Considering above references together, we can conclude that alloying of Fe with Pt brings about hybridization of d-bands resulting in the change of d-band structure, consequently Fe atoms become high-spin state showing

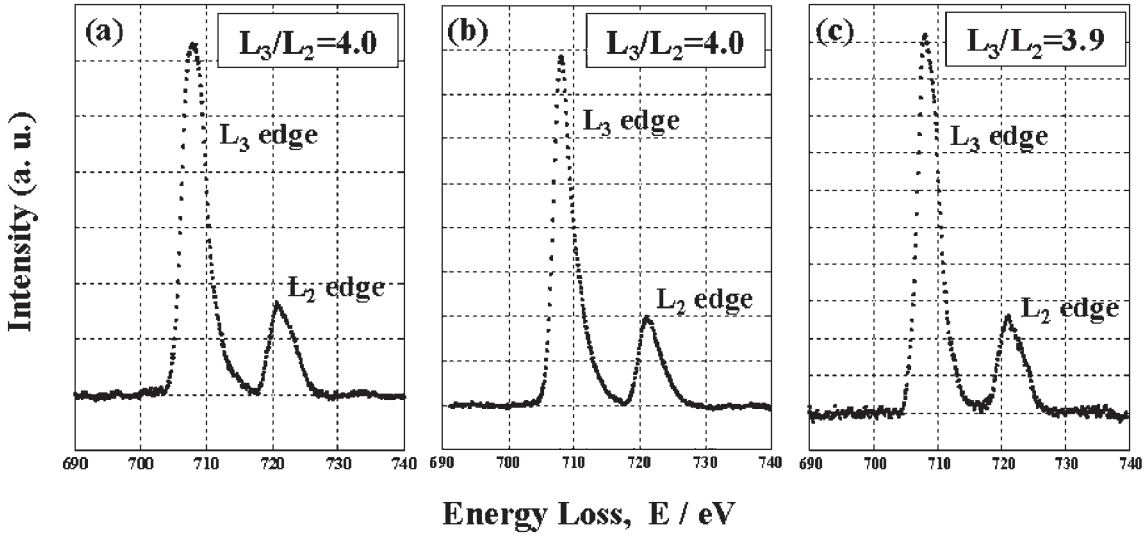

Fig. 5 Fe-$L_{2,3}$ edge in EEL spectra of (a) [MgO/Fe(1.0 nm)/Pt(0.8 nm)/MgO], (b) [MgO/Fe(0.77 nm)/Pt(0.60 nm)/MgO] and (c) [MgO/Fe(0.38 nm)/Pt(0.30 nm)/MgO]. The white-line ratios were obtained as 4.0, 4.0 and 3.9, respectively.

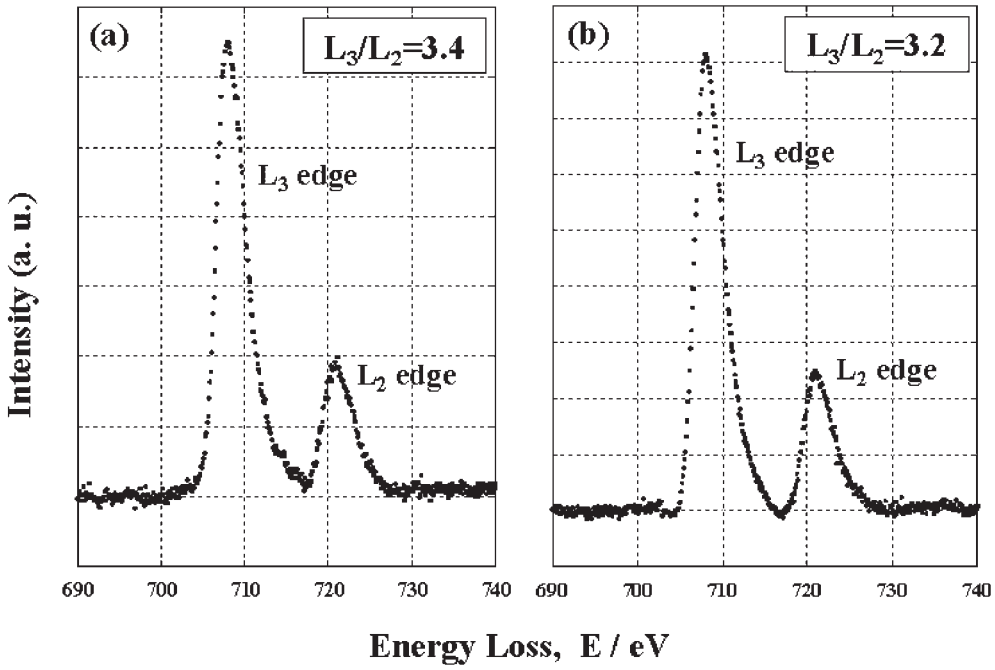

Fig. 6 Fe-$L_{2,3}$ edge in EEL spectra of (a) [MgO/Fe(1.0 nm)/MgO], (b) [MgO/Fe(2.0 nm)/MgO]. The white-line ratios were obtained as 3.4 and 3.2, respectively.

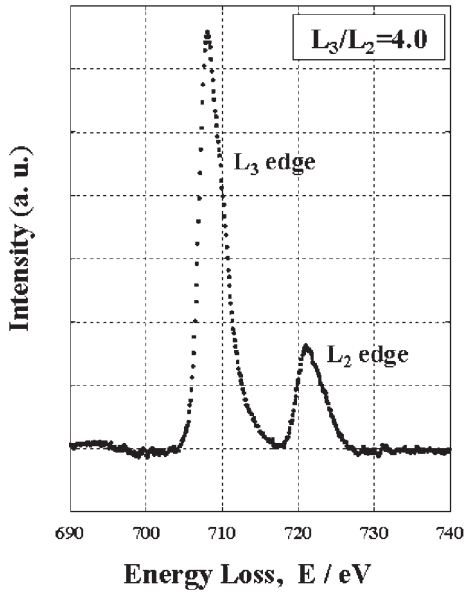

Fig. 7 Fe-$L_{2,3}$ edge in EEL spectra of [MgO/Fe(0.77 nm)/Pt(0.60 nm)/MgO] tilted to 45 degree from the incident direction of the electron beam. The white-line ratio was obtained as 4.0, that is the same value to Fig. 5(b).

larger white-line ratio.

Finally, Fig. 7 shows the Fe-$L_{2,3}$ edge in EELS of [MgO/Fe(0.77 nm)/Pt(0.60 nm)/MgO] sample tilted to 45 degree from film normal direction. The white-line ratio results in the same value as the value for non-tilted experiment (Fig. 5(b)). Although some previous reports described the dependency of incident beam direction on the EELS, that is called as "ALCHEMI" effect,[24] where the possibility of inelastic scattering of a particular atom changes due to an electron channeling effect (dynamical diffraction effect), this result suggests that white-line ratio of the present sample gives a same result independently on the incident beam direction, because the FePt clusters is very small and the MgO film is thin and not perfectly crystalline, without the channeling effect.

The results of EELS obtained from the present study imply the possibility of EELS for the detection of local structure and magnetic properties. In the near future we are going to investigate, in more detail, the relation between $L1_0$-order degree and white-line ratio using well-defined samples.

4. Concluding Remarks

FePt-MgO granular films, in which few nano-meter sized FePt clusters are dispersed with $L1_0$-ordered phase and perpendicular orientation, *i.e.* $[100](001)_{FePt} \parallel [100](001)_{MgO}$, were successfully prepared by vacuum successive deposition below 673 K. The temperature for preparation, below 673 K, is fully sustainable for the practical applications. FePt clusters were well-ordered except for the small clusters in [MgO/Fe(0.38 nm)/Pt(0.30 nm)/MgO] sample. This suggests the size effect on the stability of $L1_0$-phase of FePt clusters.

Coercivity obtained for [MgO/Fe(1.0 nm)/Pt(0.8 nm)/MgO] sample was 1.2×10^5 A/m, but larger one can be expected by some modification of the sample preparation, which we will address in near future.

White-line ratios of the Fe in [MgO/Fe/Pt/MgO] were obtained as around 4.0, independent on the incident direction of electron beam. The higher white-line ratio of Fe can be explained by its high-spin state and the change in 3d-band owing to the hybridization of d-bands between Fe and Pt atoms.

Acknowledgements

The authors appreciate Dr. K. Sato of Osaka University for his kind advice of sample preparation and the laboratory members of Prof. Mizutani of Nagoya University for their help of SQUID measurements. Dr. K. Kimoto of National Institute for Materials Science is also acknowledged for the installation of software concerning to the EELS. The present study was partly supported by a Grant-in-Aid for the Priority Area "Localized Quantum Structure" (# 751) and a Special Coordination Fund for Promoting Science and Technology on "Nano-Hetero Metallic Materials" from the Ministry of Education, Science, Sport and Culture, Japan.

REFERENCES

1) D. Weller, A. Moser, L. Folks, M. E. Best, W. Lee, M. F. Toney, M. Schwickert, J. U. Thiele and M. F. Doerner: IEEE Trans. Magn. **36** (2000) 10–15.
2) S. Iwasaki: IEEE Trans. Magn. **38** (2002) 1609–1614.
3) B. Bian, Y. Hirotsu, K. Sato, T. Ohkubo and A. Makino: J. Electron Microsc. **48** (1999) 753–759.
4) M. Watanabe, T. Masumoto, D. H. Ping and K. Hono: Appl. Phys. Lett. **76** (2000) 3971–3973.
5) T. Miyazaki, S. Okamoto, O. Kitakami and Y. Shimada: J. Appl. Phys. **93** (2003) 7759–7761.
6) C. M. Kuo and P. C. Kuo: J. Appl. Phys. **87** (2000) 419–426.
7) O. Kitakami, Y. Shimada, K. Oikawa, H. Daimon and K. Fukamichi: Appl. Phys. Lett. **78** (2001) 1104–1106.
8) Y. Endo, N. Kikuchi, O. Kitakami and Y. Shimada: J. Appl. Phys. **89** (2001) 7065–7067.
9) R. F. Egerton: "*Electron Energy-Loss Spectroscopy in the Electron Microscope*", 2'nd ed. (Plenum Press, New York, 1996).
10) D. H. Pearson, C. C. Ahn and B. Fultz: Phys. Rev. B **50** (1994) 12969–12972.
11) T. I. Morrison, M. B. Brodsky, N. J. Zaluzec and L. R. Sill: Phys. Rev. B **32** (1985) 3107–3111.
12) R. D. Leapman, L. A. Grunes and P. L. Fejes: Phys. Rev. B **26** (1982) 614–635.
13) H. Kurata and N. Tanaka: Microsc. Microanal. Microstruct. **2** (1991) 183–190.
14) Y. K. Takahashi, T. Ohkubo, M. Ohnuma and K. Hono: J. Appl. Phys. **93** (2003) 7166–7168.
15) H. Y. Pan, S. Fukami, J. Yamasaki and N. Tanaka: Mater. Trans. **44** (2003) 2048–2054.
16) S. Fukami and N. Tanaka: Philos. Mag. Lett. **84** (2004) 33–40.
17) K. Kimoto and Y. Matsui: J. Microsc. **208** (2002) 224–228.
18) K. Sato and Y. Hirotsu: Trans. Mater. Res. Soc. Jpn (2004) in press.
19) O. Kitakami and Y. Shimada: Materia Japan **40** (2001) 786–790.
20) C. Chen, O. Kitakami and Y. Shimada: J. Appl. Phys. **84** (1998) 2184.
21) C. C. Ahn and O. L. Krivanek: "*EELS Atlas*", Gatan (1983).
22) B. T. Thole and G. van der Laan: Phys. Rev. B **38** (1988) 3158–3171.
23) A. Sakuma: J. Phys. Soc. Jpn **63** (1994) 3053–3058.
24) J. Taftø and O. L. Krivanek: Phys. Rev. Lett. **48** (1982) 560–563.